Newtonian hydro-thermal fluid flow phenomena through a sudden expansion channel with or without baffles

Sandip Saha[1], Pankaj Biswas[1], Kanishka Jha[2], Apurba Narayan Das[3], Rajesh Choudhary [4,*]

[1]Dept. of Mathematics, National Institute of Technology Silchar, Silchar-788010, Assam, India

[2]Dept. of Mechanical Engineering, Lovely Professional University, Jalandhar-144001, Punjab, India

[3]Dept. of Mathematics, Alipurduar University, Alipurduar-736121, West Bengal, India

[4]Dept. of Mechanical Engineering, Sardar Vallabhbhai National Institute of Technology Surat, Surat-395007, Gujrat, India

**Corresponding author : rchoudhary@med.svnit.ac.in*

Abstract

This work aims to study the different characteristics of Newtonian fluid flow and heat transfer through a 1:3 sudden expansion channel with or without plane baffles using the finite volume method. The flow is assumed viscous, incompressible, steady, and laminar. The different characteristics of hydro-thermal fluid flow phenomena have been studied for $Re \in [0.1 - 200]$ to demonstrate the influence of the presence of baffles. The profiles of velocity, pressure, skin friction coefficient, friction factor, average Nusselt number, and pumping power have been examined for both the cases of the presence and absence of baffles. It has been observed that the hydro-thermal characteristics become more pronounced with the increase in the number of baffles. In the case of three baffles of equal length, at $Re = 200$ it is calculated that if the thickness of the baffles is same and equal to 10% of the length, then the value of Nu_{av} becomes approximately 1.2 times of that in the absence of baffle. For the same value of Re, it has been found that for the presence of one baffle of length equal to the width of the inlet section of the channel and of thickness 10% of the same, the value of Nu_{av} becomes 1.11 times of that in the absence of baffle, while in the case of three baffles of equal length and of equal thickness like the above mentioned case of one baffle, the value of Nu_{av} becomes 1.25 times of that in absence of baffle. It has also been revealed that the enhancement of thermal phenomena increases with the increase in the baffle's height.

Keywords: Baffles; newtonian fluid flow;nusselt number; pumping power; reynolds number.

NOMENCLATURE

C_p	average pressure coefficients	u_0	average velocity
c_p	specific heat capacity	ρ	density (kg/m^3)

$C_f = \frac{2\tau_w}{\rho u_0{}^2}$	local skin friction coefficient	$\eta = \frac{\mu}{\rho}$	kinematic viscosity
$d_1, d_2, d_3, d_4,$	baffle distance	$Nu = \frac{hL}{k_f}$	local Nusselt number
d_5, d_6, d_7	baffle or baffles thickness		
$ER = \frac{L_d}{L_u}$	expansion ratio	$Nu_{av} = \frac{1}{L}\int Nu\,dx$	average Nusselt number
$f = \frac{2\Delta p L_d}{L\rho u_0{}^2}$	friction factor	Δp	absolute pressure drop (Pa) = $\lvert(p_2 - p_1)\rvert$
h_i	corner vortex length	$P_p = u_0 \Delta p L_u$	pumping Power
h_u	upstream channel length	τ_w	wall shear stress
h	heat transfer coefficient	Re_{crit}	critical Reynolds number
h_1, h_2, h_3	baffle height	$Re = \frac{u_0 L_u \rho}{\mu}$	Reynolds number
k_f	thermal conductivity (W/mK)	$S_i (i = 1,2,3,4) = \frac{h_i}{L_u}$	normalized vortex length
L	downstream channel length	N	power law index
L_d	width of the channel at the outlet	$\frac{x}{h_u}$	normalize location
L_p	lower side wall width	x_1	location of generating plane
L_u	width of the channel at the inlet	u, v	velocity components along x and y directions
N_e	total number of elements	x, y	Cartesian coordinates
p	pressure (Pa)		
p_1, p_2	pressure at the inlet and outlet sections		
T	temperature (K)		

1. Introduction

Nowadays, researchers are highly engaged in studying the thermo-physical behaviour of fluid flow in different equipment's, which has made significant progress in many engineering fields [Arani *et al.,* (2017); Rahmati *et al.,* (2017); Saha *et al.,* (2023)]. Sudden expansion is a well-known problem in which the flow is expanded in an abrupt way [Karimipour *et al.,* (2015); Akbari *et al.*, 2016a, Akbari *et al.*, 2016b; Saha & Das, 2021)]. With the increase in Re, many authors, experimentally and numerically, demonstrated that two or more flow separation zones exist at the lower and upper corner walls [Cherdron *et al.,* (1974); Mukhambetiyar *et al.,* (2017)]. The works on sudden expansion channels are essential in various industries, including conversion of energy, electronic cooling equipment, mixing vessels, heat exchangers, environmental control, and chemical manufacturing [Safaei *et al.,* (2014); Al-Ashhab (2019); Torres *et al.,* (2020); Quadros *et al.,* (2020); AL-Jawary (2020); Saha,2021a, Saha ,2021b] as vortices appear after the backward-facing step and results in considerable heat loss. Therefore, it is important to understand the basic phenomenon of flow characteristics and enhancement of heat transfer through a sudden expansion channel.

Durst *et al.,* (1974) experimentally investigated the Newtonian fluid flow phenomena in a suddenly expanded channel. They stated that flow becomes asymmetric (existence of two corner vortices of different lengths) at $Re > 56$. In a sudden expansion channel, Fearn *et al.,* (1990) experimentally and numerically showed the flow symmetry, after a certain value of Re, losses its stability. Using linear stability analysis, Shapira *et al.,* (1990) studied the flow bifurcation in an expansion channel for different values of ER. They also stated that the flow losses its stability when $Re > Re_{crit}$. To investigate the influence of ER on asymmetric states, Battaglia *et al.,* (1997) conducted linear stability analysis and steady flow simulations. To determine the bifurcation point, they used bifurcation theory and stated an inverse relationship between ER and Re_{crit}. Alleborn *et al.,* (1997) also studied the linear stability analysis to clarify the effect of ER and the characteristics of flow bifurcation phenomena. Using the continuation method, the steady-state bifurcation diagrams were presented for higher values of Re. Drikakis (1997) employed various discretization schemes up to fourth order for the simulations of steady-state bifurcation characteristics in a sudden expansion channel. To compute the value of Re_{crit}, they showed that third and fourth-order finite difference schemes are very much effective. Moreover, they observed that the value of Re_{crit} decreases with the increase of ER. Soong *et al.,* (1998) numerically studied the laminar flow in a sudden expansion channel for asymmetric flow conditions and flow instability. In a two-dimensional case, complex flow patterns were identified, which are associated with unsteady and periodic solutions for large values of Re. In a sudden expansion channel, Hammed *et al.,* (1999) investigated the laminar flow by real-time digital particle image velocimetry (PIV). For different values of Re, they presented the velocity contours to observe the flow characteristics and concluded that the length of vortex varies linearly with the increase in Re.
In a suddenly expanded channel, Pinho *et al.,* (2003) investigated the pressure drop characteristics of shear-thinning laminar power-law fluids. They revealed that in the expanded section, the profile of velocity becomes parabolic for small values of Re. In a backward-facing step channel, Oder *et al.,* (2003) studied different phenomena of thermal characteristics for different values of Pr. Thiruvengadam *et al.,* (2005) studied the flow bifurcation and heat transfer characteristics in a symmetric sudden expansion channel. They found that the values of C_f and Nu_{av} were influenced significantly due to the increase in the values of Re. In 2009, Ternik studied the transition of generalized Newtonian fluids over a sudden expansion channel. They found that the increase in the values of n causes increase in recirculation length and Re_{crit}. Ternik (2010) solved the problem of the laminar flow for a wide range of Re through a 1:3 suddenly expanded channel in two-dimension. Considering

power-law index in the range 0.60 to 1.40, they obtained the recirculation length and Couette correction for power-law fluids ($n < 1$ and $n > 1$), and reported that the reattachment and detachment points are influenced by non-Newtonian viscous behaviour. In addition, for $n < 1$, they showed that the increase in the values of n causes increase in the vortex length. However, for $n > 1$, they established a linear relationship between reattachment length and the values of Re.With porous wall, Terekhov & Terekhov, 2017 numerically investigated the thermo-hydraulic phenomena of fluid flow over a backward facing channel. With or without porous block, Galuppo *et al.,* (2017) examined the turbulent flow and the thermal phenomena through a backward expansion channel. They suggested that a porous obstacle beyond the back step can be used to prevent the unexpected rise in the Nu, which is not suitable for some practical applications. Experimentally, Dyachenko *et al.,* (2019) investigated the propagation of static pressure, and the transfer of heat in the separation region formed behind the backward-facing step of a channel. They revealed that the positions of vortex generators are critical parameters that can enhance the rate of heat transfer. They have shown that the rate of heat transfer enhances, when the vortex is generated in the upstream of the channel. Chai & Song ,2019 studied the temporal stability in both the stream wise and span wise slip channels. They stated that critical values of Re are influenced by the stream wise slip and decreased by the span wise slip and concluded that flow is greatly stabilized when equal slips are placed in both the directions.

How the flow dynamics and heat transfer characteristics are affected by the presence of different forms of baffle other than rectangular one can be studied after going through this work. This work can also be generalized by taking other forms of channel embedded with baffles. The simulation results of these models can be compared with those of the case of a channel without baffle to study the effect of the presence of baffles on the flow in the channel.

The dynamics of fluid flow via a sudden expansion channel are of practical and basic interests for having numerous applications in medical research, engineering, and manufacturing processes such as electronic cooling equipment, mixing vessels, and heat exchangers. The most frequent geometry used in heat exchangers is banks of tubes, which may be found in various industrial operations including the nuclear industry. Cross flow through the banks is achieved in shell-and-tube heat exchangers by baffle plates, which are responsible for changing the direction of the flow and increases the heat exchange time between the fluid and the heated surfaces.

Till now, most of the researchers have solved problems on sudden expansion channel considering the variations in the values of ER and n. In addition, it is clear that most of the works are limited to the study of fluid flow characteristics. Only a few works have been performed on both the fluid flow and heat transfer characteristics. From the above literature survey, it has been clear that the effect of the presence of baffles on hydro-thermal flow characteristics through a sudden expansion channel has not been considered so far. This work is an extension of the study of Ternik *et al.,* (2006). They studied the evolution of two-dimensional, viscous, power-law fluid flow phenomena without considering heat transfer phenomena, and the effect of the presence of baffles. In this work, we have demonstrated the effect of baffles on different characteristics of thermo-hydraulic Newtonian fluid flow phenomena. The variations of different heat transfer characteristics of Newtonian fluid flow have been presented in the form of graphs with the variations in baffle thickness and height for different values of Re.

2. Flow geometry

Two-dimensional computational flow geometry [Ternik *et al.,* (2006)] in a symmetric sudden expansion channel in presence or absence of plane baffles have been illustrated schematically in figures 1(a-b), which is divided into three sections viz., inlet, wall and outlet sections. Flow geometry is prescribed in a Cartesian coordinate system x, y for ER = 3. Two-dimensional laminar flow in a sudden expansion channel exhibits clearly a flow transition from symmetric to asymmetric as the value of Re increases. Fluid flow boundary conditions have been taken as per the studies of Ternik *et al.,* (2006) and the thermal boundary conditions have been chosen from the work of Nasiruddin *et al.,* (2006).

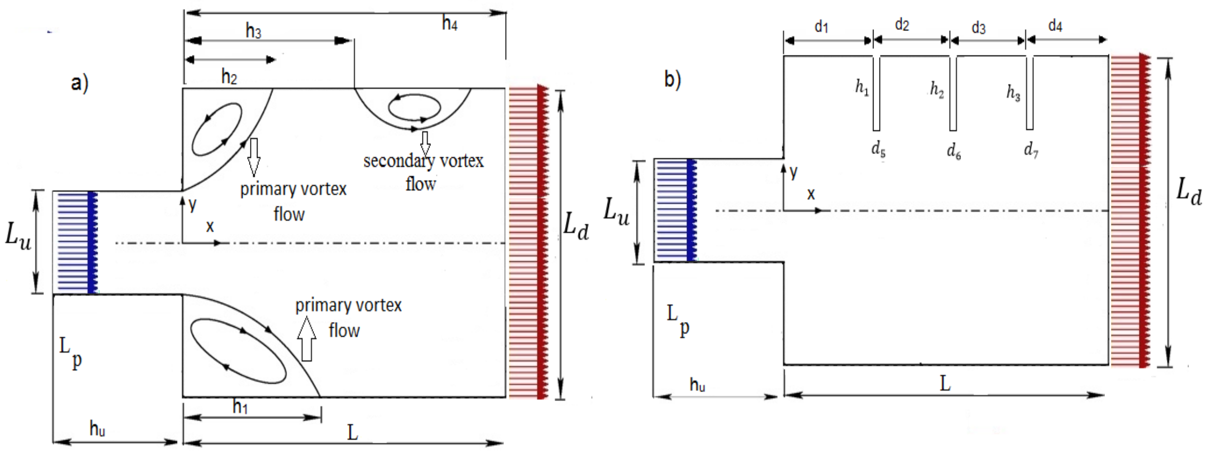

$$L = 50\,L_u \quad ER = \frac{L_d}{L_u} = 3 \quad L_u = L_p \quad 2L_u = h_u$$

Fig. 1. Schematic diagram in (a) absence of baffles, (b) presence of three baffles where, $d_1 = d_2 = d_3 = d_4$.

3. Formulations

Newtonian fluid flow in a sudden expansion channel is associated with the following equations [Saha *et al.*,2020; Saha *et al.,* 2022]:

Equation of continuity:

$$\nabla.\mathrm{R} = 0 \tag{1}$$

Equation of x-momentum:

$$(\mathrm{R}.\nabla)\mathrm{u} = \eta\nabla^2\mathrm{u} - \frac{1}{\rho}\mathrm{p_x} \tag{2}$$

Equation of y-momentum:

$$(R.\nabla)v = \eta\nabla^2 u - \frac{1}{\rho}p_y \quad (3)$$

Energy equation:

$$(R.\nabla)T = \frac{k_f}{\rho c_p}\nabla^2 T \quad (4)$$

With $R = (u, v)$and $\nabla = i\frac{\partial}{\partial x} + j\frac{\partial}{\partial y}$.

3.1 Boundary Condition

i) Inlet section: For x/L_u=-2 and $-0.5<y/L_u<0.5$, at the inlet section, inflow velocity ($u = u_0$) has been imposed, with $u_0 \in$ [0-0.178] m/s and $0 \le Re \le 200$. At the channel inlet, the temperature of the working fluid has been set at 27^0.
ii) Outlet section: For x/L_u= 50, an outflow boundary condition (all flow properties have zero gradients, and the flow is normal to outflow surface) has been applied in the outlet section.
iii) Wall sections: At the channel walls, no-slip ($u_x = 0, v_x = 0$) and no-penetration ($u_y = 0, v_y = 0$) boundary conditions are assumed, to mean that fluid flows steadily through the channel. The no-slip condition for viscous fluids represents that the fluid has no velocity relative to the boundary. Arbitrarily, the walls of the computational domain have been kept at 102^0C.

3.2. Computational Procedures, Grid Study, and Validation of Code

Ansys Fluent has been used for simulation and visualization purposes. All the variables defined at the centre of the control volume populating the physical domain have been considered, when solving the governing equations using FVM [Youcef *et. al.,*2019, Youcef & Saim 2021)]. Each equation is integrated over each control volume to provide a discrete equation that links the variable at the volume's centre to its neighbours. Despite some compelling features of the finite volume method (e.g., the resulting solution satisfies the conservation of quantities such as mass, momentum, and so on), lower order interpolation of the convective terms in the governing equations causes different unwanted numerical effects (e.g., artificial diffusion). To avoid those, the QUICK scheme [Leonard's (1979)] has been utilized for spatial discretization of convective terms in a momentum equation. It is an upwind scheme (two upstream points and one downstream point) that is accurate up to 3rd order for advection terms but up to 2nd order for all other terms (diffusion terms). SIMPLEC algorithm [van Doormaal *et al.,* (1984); Ternik *et al.,* (2006)] resolves the coupling between velocity and pressure. The convergence criteria have been set as 10^{-6}, 10^{-6}, and 10^{-9} for continuity, momentum, and energy equations respectively.

At Re=60, the grid test has been performed for both the cases of smooth channel and the baffled channel to study the effect of mesh size [illustrated in figures. 2(a-b)]. To find a numerical solution through discretization of the governing differential equation, the solution is dependent on the number of grid points. Generally, when we increase the number of grid points, the solution becomes accurate, but main problem is that to what extent we should increase this number of grid point. When our solution does not change with the change in the number of grid points, we select that very number of cells to continue, which means after a certain number of cells, the trend of graph become linear. For smooth channel, we start our calculation with 15,000 number of cells. It has been found that if the number of cells is greater than 15,000, the value of C_p increases continuously, but the graph of C_p becomes linear (marked by circle in the graph), when the number of cells exceeds 60,820. In addition, for 60,820 number of cells and 240,000 number of cells, the solutions are same, it means 60,820 number of cells are optimum for the solution and the solution is not going to change further with the

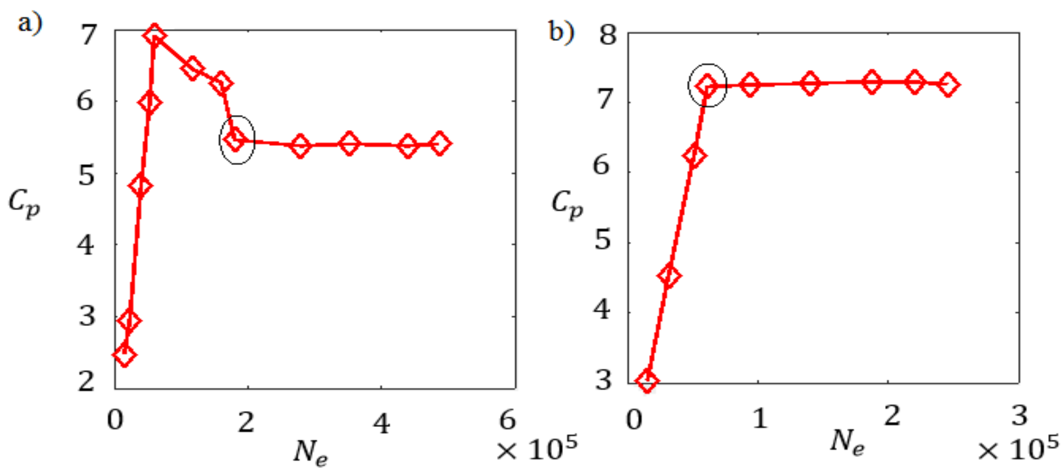

Fig. 2. At $Re = 60$, variations of C_p vs. N_e for (a) no baffle, (b) three baffles cases.

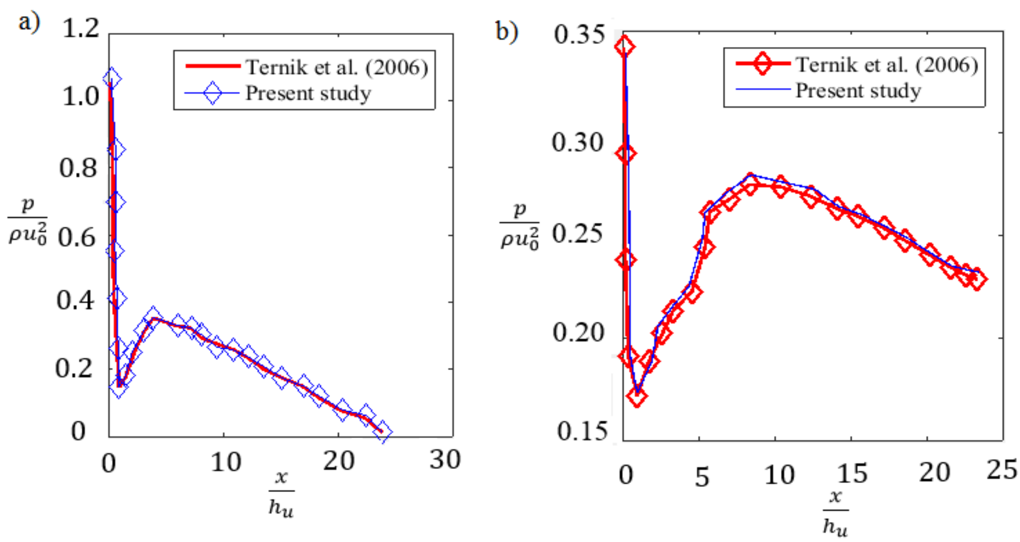

Fig. 3. Plots of $\frac{p}{\rho u_0^2}$ vs. $\frac{x}{h_u}$ at (a) $Re = 50$, (b) $Re = 100$ along the centerline.

increase in the number of grid points. So 60,820 number of cells are optimum grid points [figure. 2(a)] for our solution. Again, for a channel with three baffles, we start our calculation with 15,000 number of cells. It has been found that when the number of cells are greater than 15,000, the value of C_p increases continuously, but if the number cells exceeds 172, 680, the graph of C_p become linear (marked by circle in the graph). Also, further increase in the value of the number of cells up to 496, 888, the same linear trend has been observed. So 172, 680 number of cells are optimum grid points [figure. 2(b)] for our solution. The code validation has been done with the studies of Ternik *et al.,* (2006) by comparing the results of normalized pressure profile at $Re = 60$ [figure. 3(a)] and $Re = 100$ [figure. 3(b)], which shows a good agreement [figures. 3(a-b)] of those with the present models and provides us enough confidence to carry forward the present work. The table 1 show the % error between the present study and the work of Ternik *et al.,* (2006). The whole computation has been segregated into two different parts with the aid of fine mesh as shown in figure. 4.

Table 1. % error of Ternik *et al.* (2006) and Present study at $Re = 100$

	Ternik *et al.* (2006)	Present study	
$\frac{x}{h_u}$	$\frac{p}{\rho u_0^2}$	$\frac{p}{\rho u_0^2}$	% error$=\frac{\lvert \text{Ternik } et\ al.\ (2006) - \text{Present study}) \rvert}{\text{Present study}} \times 100$
0.097276	0.342043	0.342101	0.01693
0.194553	0.238183	0.237989	0.08132
1.750973	0.188741	0.188751	0.00498
4.571984	0.222694	0.22251	0.08270
8.365759	0.27481	0.275453	0.23353
17.2179	0.253498	0.253593	0.03733
22.56809	0.23081	0.230853	0.01871
Total % error= 0.39			

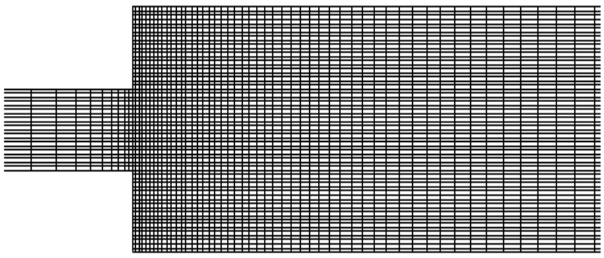

Fig. 4. Mesh geometry in absence of baffles.

4. Results and Discussions

This section describes the influence of the absence and presence of baffles on different characteristics of hydro-thermal flow phenomena with the variations in baffles height, thickness and Re.

4.1. Effect of Presence or Absence of Baffles

Velocity streamlines have been shown in figures. 5(a-d) for different values of Re in the case of smooth channel. When the flow passes through the channel expansion, with the increase in inlet velocity, some vortices arise in the low-pressure regions [figures. 5(a-d)]. In addition, the vortices are strengthened with the increase in the inlet velocity, and those move towards the outlet of the channel. It is seen that indistinguishable equal corner vortices are exist at $Re = 0.99$. It is also found that as Re is increased to 30, the vortices in both the corners are increased in size. Many authors [Samingue *et al.,* (2010); Quadros *et al.,* (2019)] stated that if Re exceeds Re_{crit} , the flow loses its symmetry (i.e., flow bifurcation starts) and reaches its asymmetric state. But it is to be mentioned that for non-zero values of Re, the flow never be symmetric, and this is observed more clearly if Re exceeds Re_{crit} as the flow lost its symmetry highly then [as can be seen in figures. 5(c-d) and figure. 6]. For creeping flow [figure. 5(a)], fluid flow starts to deviate from the axial position, x = $-2h_u$, before the expansion plane. In figure. 6, it is found that for $Re \in [0.1 - 59.8]$, the length of the corner vortices at the lower and upper walls are almost equal. At $Re = 0.99$, two vortices are found at each of the corner walls, see figure. 5(a). In figure. 6, it is found that for $Re \in [0.1 - 59.8]$ corner vortices are developed linearly. However, for $Re > 59.8$, the size of one corner vortex starts to increase, while that of other corner vortex starts to decrease showing that the symmetry of flow changes into a stable asymmetric flow [figures. 5(c-d)]. With the increase in Re, more than two separate zones are found at the channel walls, as shown in figures. 5(c-d). The figure. 7 represents the influence of no baffle [figure. 7(a)], presence of one baffle [figure. 7(b)], two baffles [figure. 7(c)] and three baffles [figure. 7(d)] on the vortex flow patterns. The flow separation causes a recirculation zone in the downstream of the baffles, as the baffles prevent the boundary layer development. As a consequence, the number of vortices as well as the length of the vortices increase. It found in the figures. 7(a-d) that the velocity streamlines become slightly pronounced for the presence of baffles. In addition, it has also been observed that vortices arise in the base of the baffles.

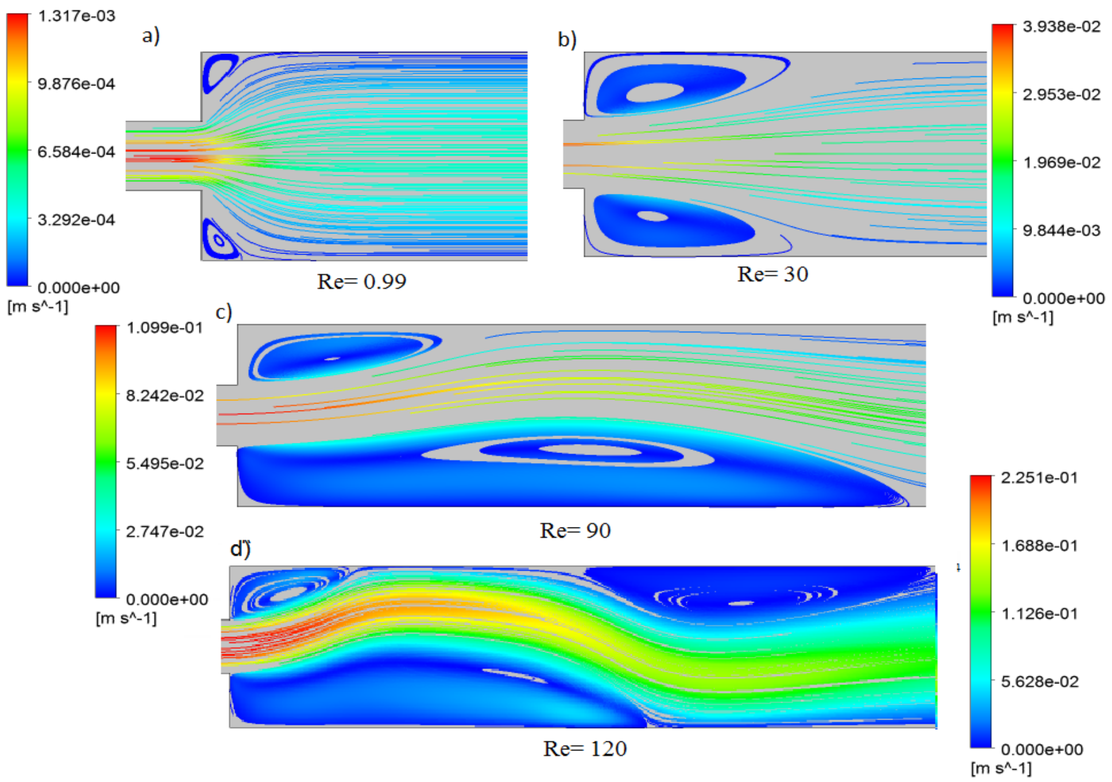

Fig. 5. Velocity streamlines for various Re in absence of baffles.

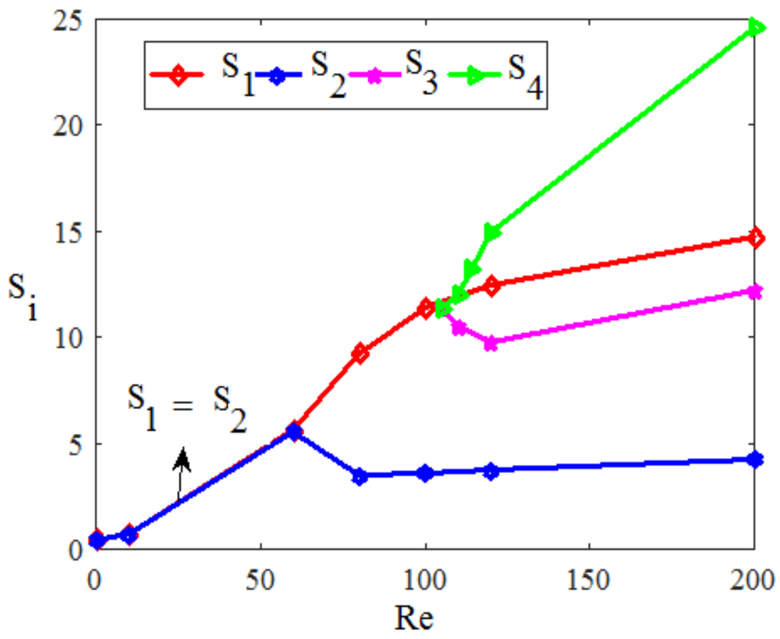

Fig. 6. Variations of normalized vortex length for various Re in absence of baffles.

Moreover, it is found that the number of vortices increases with the increase in the number of baffles in the upper wall of the channel, as expected [figure. 7]. The profile of the temperature contours have been shown in figures. 8(a-d) at $Re = 90$ in the cases of no baffle [figure. 8(a)], presence of one baffle [figure. 8(b)], two baffles [figure. 8(c)] and three baffles [figure. 8(d)]. As expected, the rate of heat transfer increases due to the increase in the length of the vortices. As represented in figures. 8(a-d), there is barely a little difference in temperature among those cases, except near the baffles.

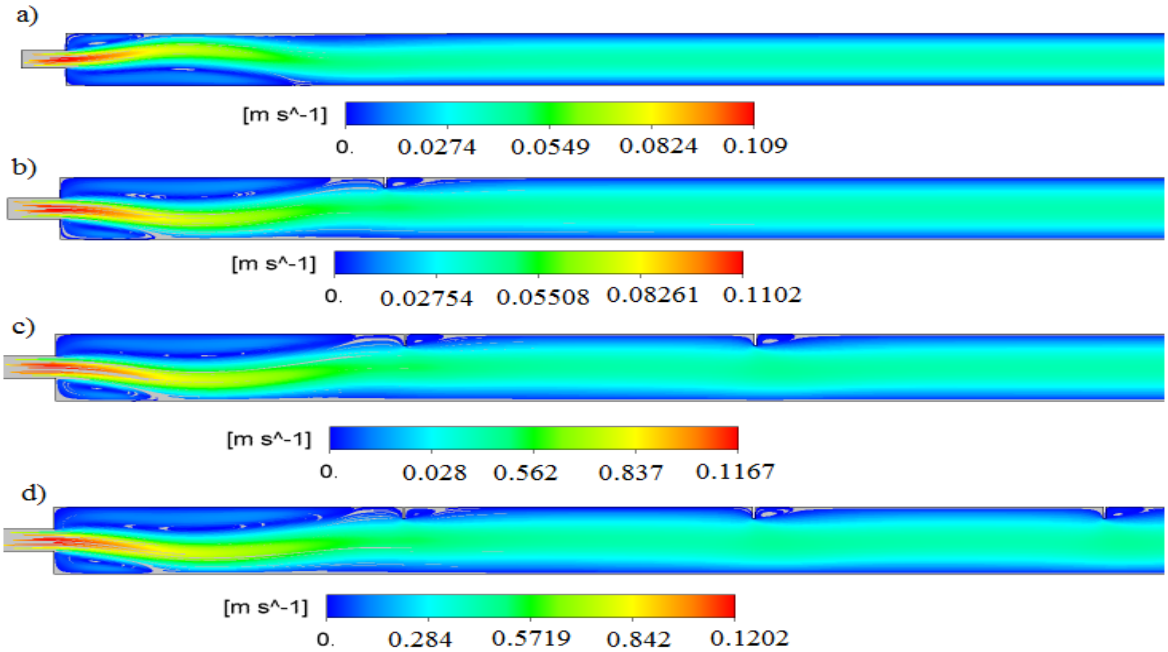

Fig. 7. Velocity streamlines for $Re = 90$ in case of absence of baffles (a), presence of one baffle (b), two baffles (c) and three baffles, where $h_1 = h_2 = h_3 = \frac{L_u}{2}$, and $d_5 = d_6 = d_7$.

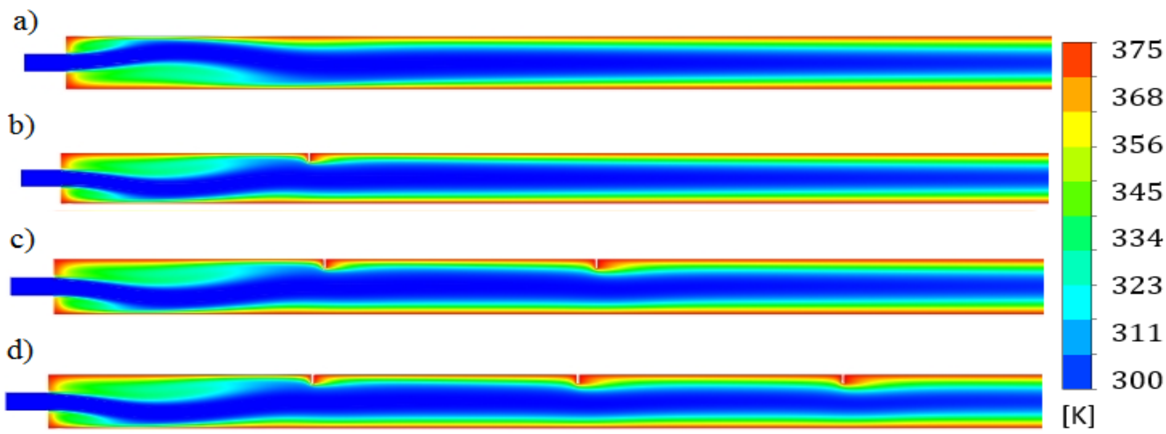

Fig. 8. Temperature profiles for $Re = 90$ in case of (a) absence of baffles, presence of (b) one baffle, (c) two baffles and (d) three baffles, where $h_1 = h_2 = h_3 = \frac{L_u}{2}$, and $d_5 = d_6 = d_7$.

In the absence of baffles, the figure. 9(a) presents the velocity distribution along the centreline for different values of Re. We also note that fluid flow experiences a significant decrease due to the sudden expansion after the expansion zone. Velocity overshoot is observed at the downstream of the expansion portion for higher values of Re. It is found that velocity overshoot remains complicated and diminishes slowly with the increase in Re. At different locations of the downstream section, the centreline velocity distribution is characterized by a monotonic approach of fully developed flow conditions. The figure. 9(b) shows the pressure distribution, which follows the flow velocity profile along the centreline. With the increase in Re, the pressure attains its maximum value at the entrance of the downstream section, and afterward, it gradually decreases as the flow proceeds towards the outlet

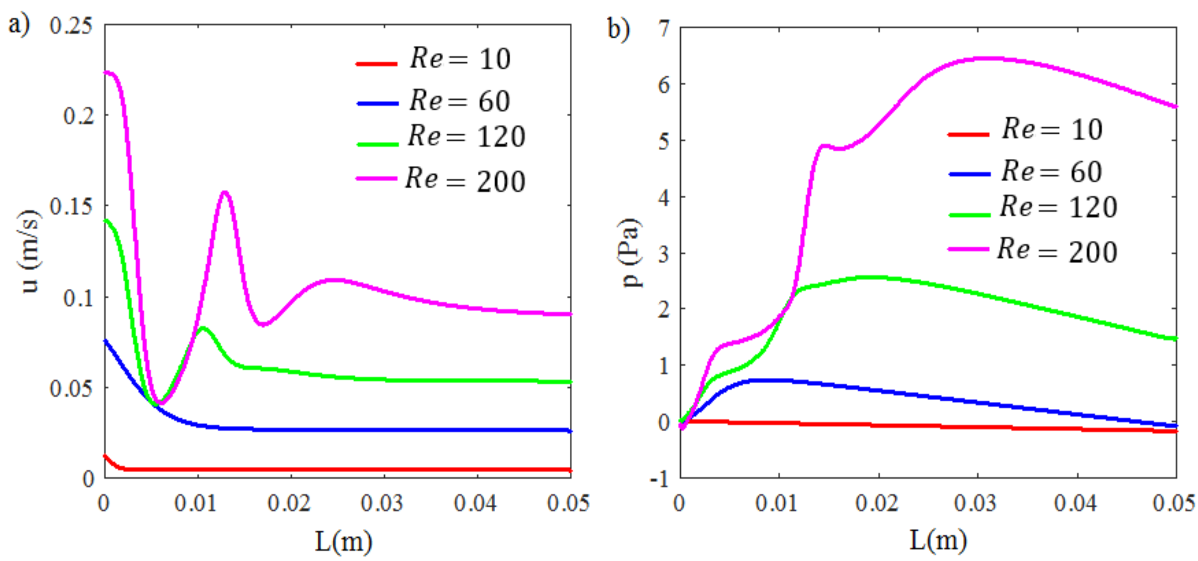

Fig. 9. Plots of (a) velocity and (b) static pressure profiles at various Re in absence of baffles.

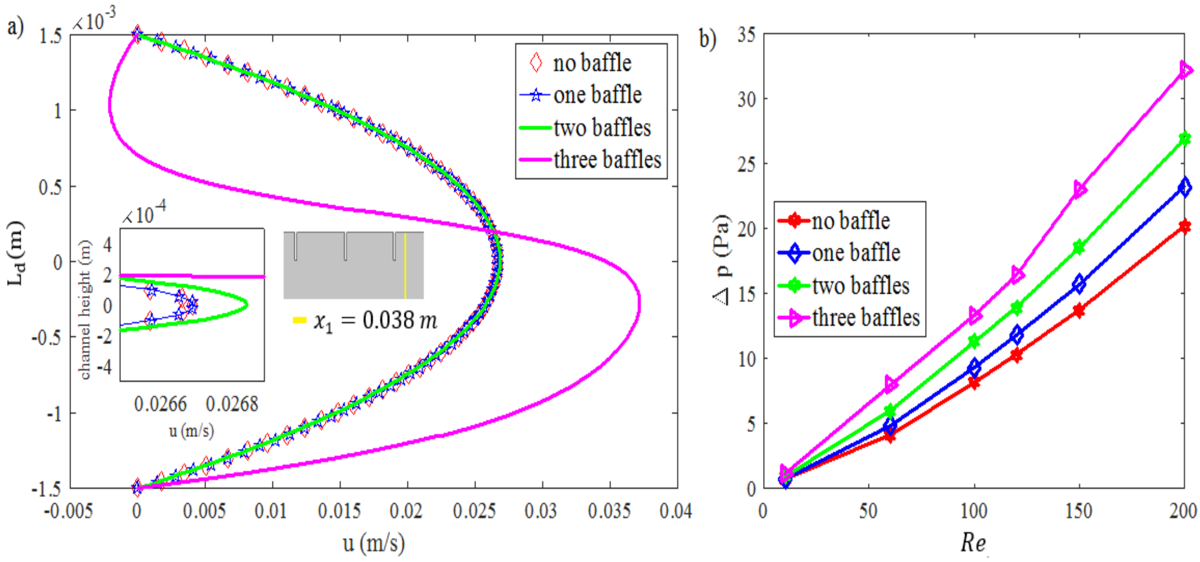

Fig. 10. Plots of (a) velocity profiles at Re= 60, $x_1 = 0.038\,m$ and variations of (b) Δp at various Re.

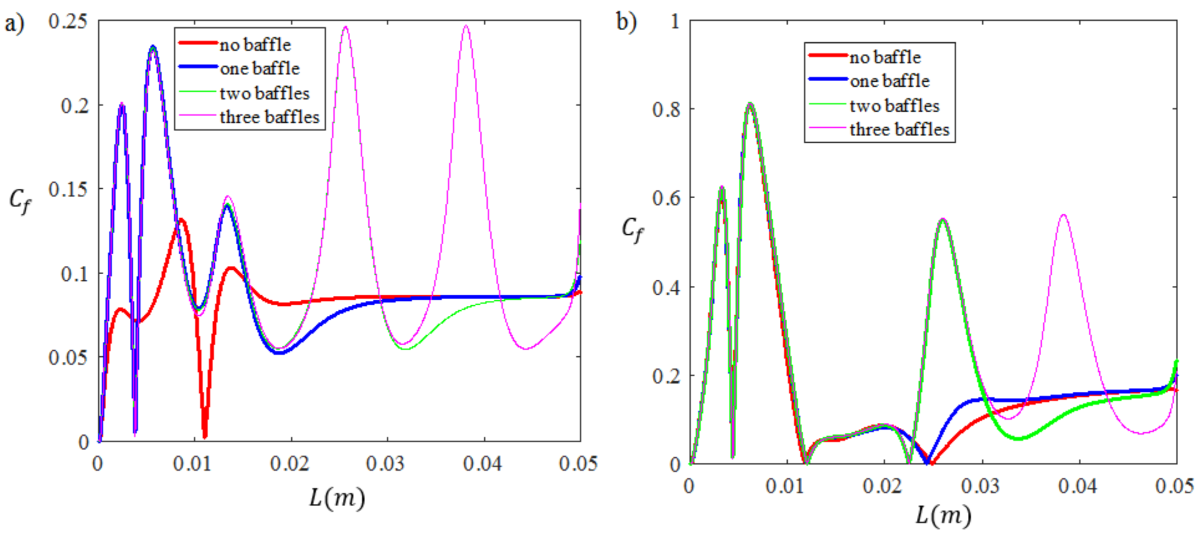

Fig. 11. Profiles of C_f at (a) Re= 100 and (b) 200 for various cases.

section of the channel. Secondary vortex flow [figure. 5(d)] has a remarkable effect on the centreline velocity for the Newtonian fluid flow and the first peak in the velocity, which appeared for $Re > 120$, causes the existence of primary vortex flow [figure. 9(a)]. Moreover, it is found that the second peak of the velocity is much smaller than the first one because the fluid flow gradually approaches the fully developed flow conditions. At higher values of Re, the variation of pressure distribution remains complex and causes the existence of different lengths of vortices at the lower and upper corner walls [figure. 9(b)]. At $Re =$ 60 and $x_1 = 0.038\,m$, the figure. 10(a) presents the variation of velocity plots. It is observed that the velocity becomes more pronounced as the number of baffles in the channel increases. At $x_1 = 0.038\,m$ and for the presence of three baffles, velocity profiles become more pronounced and of different trends because near the third baffle, the velocity increases after hitting the baffle. The location of the generating plane $(x_1) = 0.038\,m$ is far away from the locations of first and second baffles. However, the location of the generating plane, $x_1 = 0.038\,m$ is much closed to the location of third baffle. For the third baffle and at $x_1 = 0.038\,m$, different trends of velocity profile (wavy shape) is observed. This is happened as after hitting the tip of the third baffle, the flow changes its behaviour for which it looks like band wave shape and after hitting the baffle, the flow moves faster with high velocity towards the outlet of the channel.

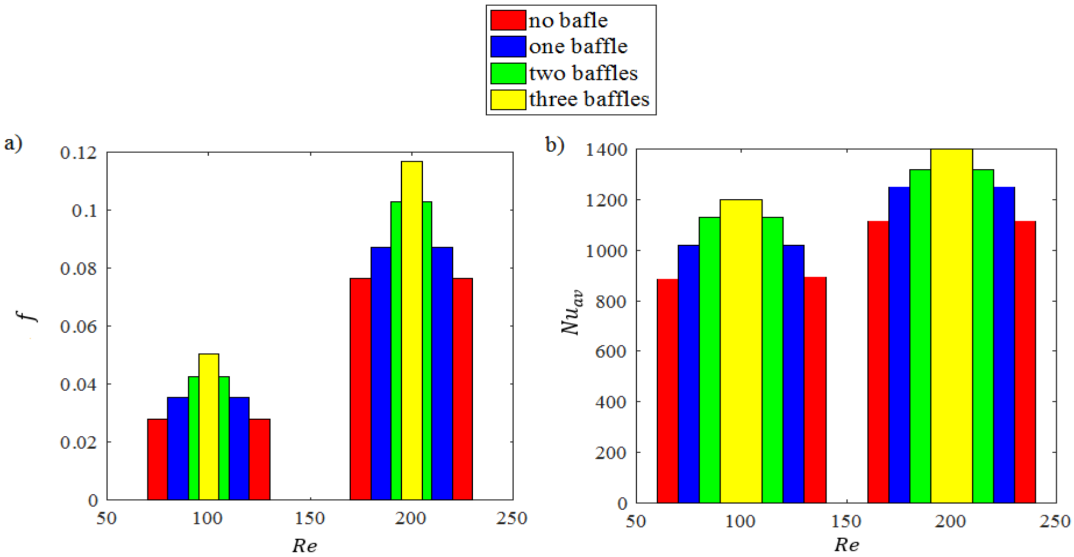

Fig. 12. Variations of (a) f, (b) Nu_{av} at various Re.

The plots of Δp have been presented for the cases of no baffle, one baffle, two baffles, and three baffles [figure. 10(b)]. It has been found that the value of Δp increases with the increase in the number of baffles and Re. It has also been revealed that the baffles interrupt the development of the boundary layer, which causes the existence of vortices near the baffles. Furthermore, at $Re = 200$ and in the case of presence of three baffles, it has also been found that value of Δp become 1.59 times of that of the case of smooth channel. For different values of Re, the figure. 11 depicts the plot of C_f in both the cases of no baffle and the presence of baffles. It has been found that the curve of C_f shows a nonlinear character at higher values of Re. It has also been found that the values of C_f become higher as compared to the case of no baffle [figures. 11(a-b)].For different values of Re, the variation in f in the presence or absence of baffles has been presented in the figure. 12(a). In presence of baffles, it has been studied that an increase of the length of vortices causes the decreases of the values of f.

Due to the increase in Δp, it has also been demonstrated that the trend of f becomes more significant in the presence of three baffles as compared to no baffle and one baffle cases [figure. 12(a)]. It is also investigated that the value of f remains higher at the higher values of Re because fluid with high velocity remains in contact with the surface walls completely. Furthermore, the C_f curve diminishes with the increase of Re as the fluid does not remain in contact completely with the channel walls. For different cases of the presence of the baffles, the variation in Re with the variations in Nu_{av} are shown in the figure. 12(b).

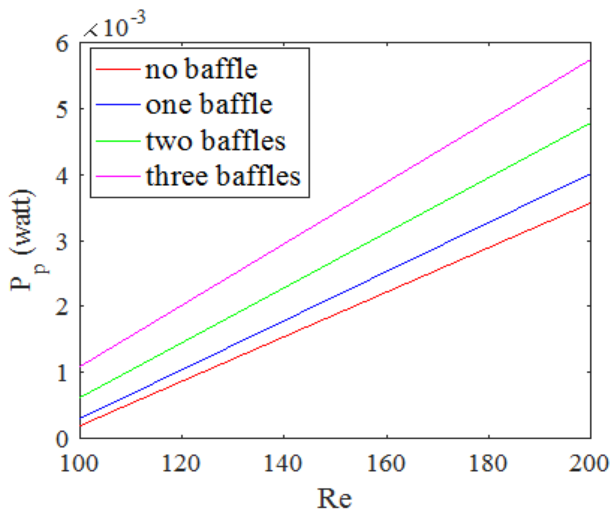

Fig. 13. Plot of P_p for various Re.

It has been found that the value of the Nu_{av} increases when the number of baffles increases. It is also evident that an increase of Re causes the increase in the values of Nu_{av}. At $Re = 200$, it has been found that in the case of one baffle ($h_1 = L_u, d_5 = 0.1\ L_u$), Nu_{av} becomes 1.11 times of that of the no baffle case, while in the case of three baffles ($h_1 = h_2 = h_3 = L_u, d_5 = d_6 = d_7 = 0.1L_u$), Nu_{av} becomes 1.25 times of that of the no baffle case. The figure. 13 presents the pumping power for different values of Re in the presence or absence of baffles. Strong pumps are required to obtain the suitable fluid velocity, and it is revealed that in the case of three baffles, 1.66 times pumping power is needed than the case of no baffle.

4.2. Effect of Baffles Thickness and Height

For various Re, the figures. 14 (a-b) show the effect of baffles thickness on heat transfer characteristics such as f and Nu_{av}. It is observed that an increase in thickness from 0.05 h_1 to 0.1 h_1, induces a decrease in the recirculation length, which causes an increase in the value of f. Therefore, an increase in mixing causes the increase of Nu_{av}. It has been found that the value of f increases with the increase in the number of baffles, as shown in the figure. 14(a). Moreover, an increase in the pressure drop causes decrease in the fluid momentum; consequently, fluid encounters the upper wall. For baffles thickness, $d_5 = d_6 = d_7 = 0.05h_1$ and $d_5 = d_6 = d_7 = 0.1h_1$, variation of Nu_{av} with Re along with the lower wall has been shown in the figure. 14(b). Heat transfer augmentation is found with the increase in baffles thickness; therefore, baffle thickness plays a crucial role in the thermal flow parameters. At $Re = 200$, it is calculated that when $d_5 = d_6 = d_7 = 0.1h_1$ then the value of Nu_{av} becomes approximately 1.04 times of that for the case, $d_5 = d_6 = d_7 = 0.05h_1$. Along the lower wall, variations in Nu_{av} and f have been shown in the figures. 15(a-b) for different values of Re. It is revealed that an increase in the baffle height induces increase in the vortex length, which causes increase in the values of f and Nu_{av}. Furthermore, for baffle height, $h_1 = h_2 = h_3 = 1.3L_u$, it has been found that the value of Nu_{av} becomes approximately 1.28 times and 1.066 times of that of the smooth channel and for $h_1 = h_2 =$

$h_3 = L_u$. Therefore, from the figures. (14-15), it has been concluded that enhancement of heat transfer becomes more pronounced with the variation in baffles height than with the variation in baffles thickness as due to increase in the baffle thickness, fluid remains at its tip and chance to contact its base reduces. However, if the height of baffle increases, fluid flows directly towards the nearby base of the baffle.

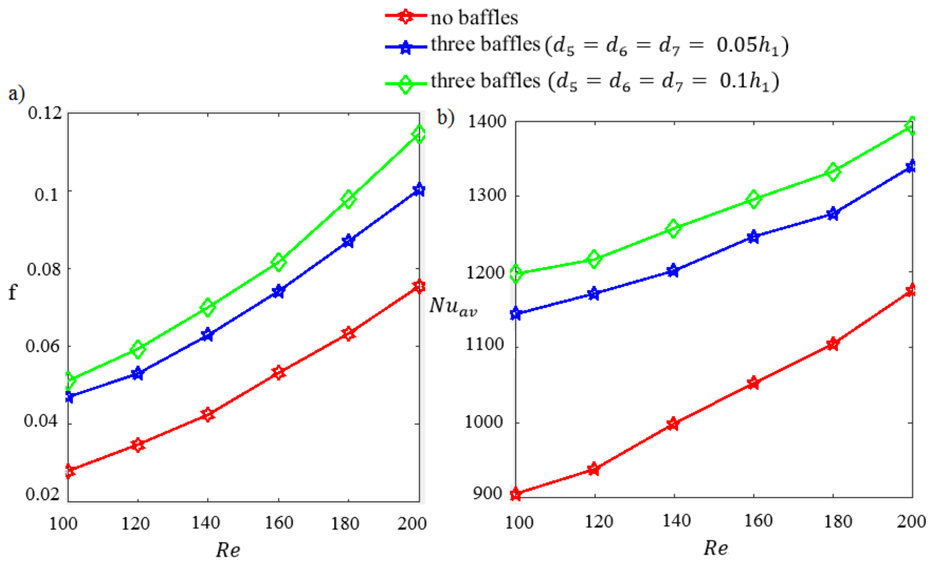

Fig. 14. Variations of (a) f, (b) Nu_{av} at various Re, where, $h_1 = h_2 = h_3 = L_u$.

5. Conclusions

Problem of flow bifurcation transition and heat transfer characteristics through a 1:3 sudden expansion channel in the presence and absence of plane baffles has been solved numerically. Effect of the variation in the values of Re on recirculation characteristics and velocity profiles of viscous, steady, incompressible, and laminar flow have been studied. Simulated results associated with the

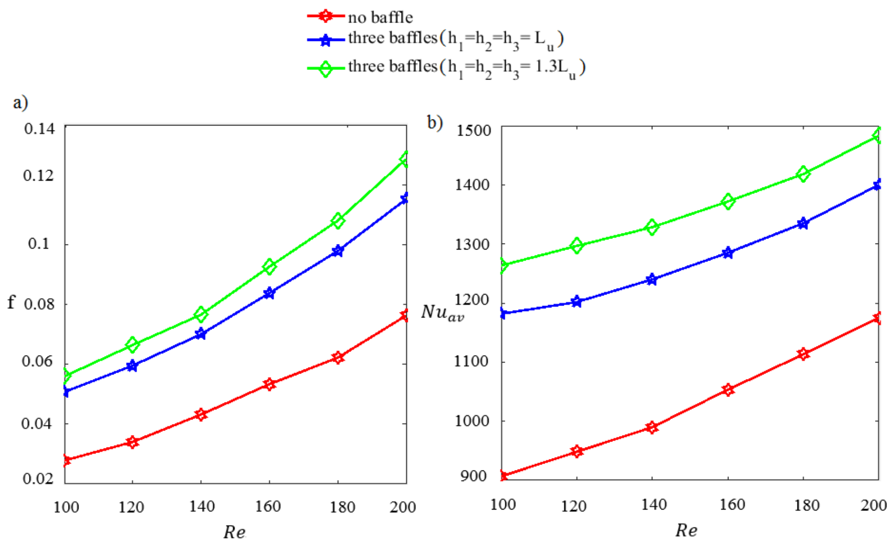

Fig. 15. Variations of (a) f, (b) Nu_{av} at various Re, where, $d_5 = d_6 = d_7 = 0.1\ L_u$.

variations in the parameters have been discussed in detail and presented graphically showing that how the presence of baffles affected several results of the case of the smooth channel. Finally, we conclude that:

a. For a smooth channel, we start our calculation with 15,000 number of cells arbitrarily. It has been found that with the increase in the number of cells, the value of C_p increases continuously, and the graph of C_p becomes linear (marked by circle in the graph), when the number of cellsis greater or equal to 60,820. This means that 60,820 number of cells are optimum for the solution, and for a channel with three baffles, we again start our calculation with 15,000 number of cells. It has been found that if the number of cells increases further, the value of $C_p$increases continuously, but if the number cells exceeds 172, 680, the graph of C_p become linear (marked by circle in the graph). So 172, 680 number of cells are optimum grid points for our solution.

b. Though many authors stated that if Re exceeds Re_{crit} , the flow loses its' symmetry (i.e., flow bifurcation starts) and reaches its asymmetric state. But the fact is that for non-zero values of Re, the flow never be symmetric, and this is observed more clearly if Re exceeds Re_{crit} as the flow lost is symmetry highly then.

c. It has been demonstrated that hydrothermal flow characteristics become more pronounced with the increase in the number of baffles. It has been found that the value of the Nu_{av} increases when the value of Re and the number of baffles increases. At $Re = 200$ and in the case of three baffles, it is calculated that when the thickness of the baffle is equal to 0.1 $h_1$then the value of Nu_{av} becomes approximately 1.2 times of that of the case of no baffle.

d. At $Re = 200$ and for $h_1 = h_2 = h_3 = 1.3\, L_u$, it is investigated that the value of Nu_{av} becomes approximately 1.28 times of that of the case of no baffle. .It is revealed that in the case of three baffles, 1.66 times pumping power is needed as compared to the no baffle case. It has also been concluded that the enhancement of thermal phenomena is clear when baffle height is considered instead of baffle thickness.

ACKNOWLEDGEMENTS

Authors are grateful for the valuable comments made on the earlier version of this work by the reviewers, which lead to an overall improvement of the work.

References

Akbari, O. A., Karimipour, B., Toghraie, D., Semiromi, A., Safaei, R.M., Alipour, H., Goodarzi, M. & Dahari, M. (2016a) Investigation of Rib's height effect on heat transfer and flow parameters of laminar water-Al_2O_3nanofluid in a two dimensional rib-micro-channel, Appl. Math. Comput, 290: 135-153.

Akbari, O. A., Toghraie, D. & Karimipour, A. (2016b) Numerical simulation of heat transfer and turbulent flow of water nanofluids copper oxide in rectangular microchannel with semi attached rib, Adv. Mech. Eng, 8(4): 1-25.

AL-Jawary, M. (2020) Three iterative methods for solving Jeffery-Hamel flow problem. Kuwait Journal of Science, 47(1): 1-13.

Al-Ashhab, S. (2019) Asymptotic Behaviour and Existence of Similarity Solutions for a Boundary Layer Flow Problem. Kuwait Journal of Science, 46(2): 13-20.

Alleborn, N., Nandakumar, K., Raszillier, H. & Durst, F. (1997) Further contributions on the two-dimensional flow in a sudden expansion. J. Fluid Mech. 330: 169-188.

Arani, A. A.A., Akbari, A. O., Safaei, R. M., Marzban, A., Alrashed, G., Ahmadi, R. & Nguyen, K. T. (2017) Heat transfer improvement of water/single-wall carbon nanotubes (SWCNT) nanofluid in a novel design of a truncated double layered micro-channel heat sink. Int. J. Heat Mass Tran, 113: 780-795.

Battaglia, F., Tavener, J. S., Kulkarni, K. A. &Merkle, L. C. (1997) Bifurcation of low Reynolds number flows in symmetric channels, AIAA Journal, 35: 99-105.

Cherdron, W., Durst, F. & Whitelaw, H. J. (1974) Asymmetric flows and instabilities in symmetric ducts with sudden expansions. J. Fluid Mech, 84: 13-31.

Chai, C. & Song, B. (2019) Stability of slip channel flow revisited, Phys. Fluids, 31: 84-105.

Drikakis, D. (1997) Bifurcation phenomena in incompressible sudden expansion flows. Phys. Fluids, 9: 76-87.

Durst, F., Melling, A. & Whitelaw, H. J. (1974) Low Reynolds number flow over a plane symmetric sudden expansion. J. Fluid Mech, 64: 111-128.

Dyachenko, U. Y., Zhdanov, L. Y., Smulskii, I. Y. & Terekhov, I. V. (2019) Experimental investigation of heat transfer in the separation zone behind a backward-facing step in the presence of tabs. ThermophysAeromech, 26: 509-518.

Fearn, M. R., Mullin, T. &Cliffe, K. A. (1990) Nonlinear flow phenomena in a symmetric sudden expansion. J. Fluid Mech, 211:595-608.

Galuppo, C. W. & De Lemos, M. J. S. (2017) Turbulent heat transfer past a sudden expansion with a porous insert using a nonlinear model. Numer Heat Transf Part Appl, 71: 290-310.

Gürcan F. (2003) Effect of the Reynolds Number on Streamline Bifurcations in a Double-Lid-Driven Cavity with Free surfaces, Computers and Fluids, 32(9): 1283-1298.

Hammad K. J., Otugen, V. M. & Arik, E. B. (1999) A PIV study of the laminar axisymmetric sudden expansion. Flow Experiments in Fluids, 26: 266-272.

Karimipour, A., Alipour, H., Akbari, O. A., Toghraie, D., Semiromi, M. &Esfe, H. (2015) Studying the effect of indentation on**Karimipour** flow parameters and slow heat transfer of water-silver nanofluid with varying volume fraction in a rectangular Two-Dimensional microchannel, Ind. J. Sci. Tech, 8(15): 51-70.

Leonard, P.B. (1979) A stable and accurate convective modeling procedure based on quadratic upstream interpolation, Comput. Methods Appl. Mech. Eng, 19: 59-98.

Mukhambetiyar, A., Jaeger, M.& Adair, D. (2007) CFD Modelling of Flow Characteristics in Micro Shock Tubes, Journal of Applied Fluid Mechanics, 10(4): 1061-1070.

Nasiruddin, M.H.& Siddiqui, K. (2006) Heat Transfer Augmentation in a Heat Exchanger Tube Using a Baffle, Int. J. Heat Fluid Flow, 28(2): 318-328.

Oder, J., Tiselj, I., Jger, W., Schaub, T., Hering, W. &Otic, I. (2020) Thermal fluctuations in low-Prandtl number fluid flows over a backward facing step. NuclEng Des, 359: 1104-1116.

Pinho, T. F., Oliveira, J. P. & Miranda, P. J. (2003) Pressure losses in the laminar flow of shear-thinning power-law fluids across a sudden axi-symmetric expansion. Int. J. Heat Fluid Flow, 24: 747-761.

Quadros, D. J., Khan, A.S.& and Antony, J.A. (2019) Study of Effect of flow parameters on base pressure in a suddenly expanded duct at supersonic Mach number regimes using CFD and design of experiments, Journal of Applied Fluid Mechanics, 11: 483-496.

Quadros, D. J. & Khan, A. S. (2020) Prediction of Base Pressure in a Suddenly Expanded Flow Process at Supersonic Mach Number Regimes using ANN and CFD. Journal of Applied Fluid Mechanics, 13: 499-511.

Rahmati, R. A., Akbari, O. A., Marzban, A., Toghraie, D., Karimi, R. & Pourfattah, F. (2017) Simultaneous investigations the effects of non- Newtonian nanofluid flow in different volume fractions of solid nanoparticles with slip and no-slip boundary conditions. Thermal Sci. Eng. Progress, 5: 263-277.

Safaei, R. M., Togun, H., Vafai, K., Kazi, N. S. &Badarudin, A. (2014) Investigation of heat transfer enchantment in a forward-facing Contracting channel using FMWCNT nanofluids. Numer. Heat Tran, 66: 1321-1340.

Saha, S., Biswas, P. & Nath, S. (2020) Bifurcation phenomena for incompressible laminar flow in expansion channel to study Coanda effect, Journal of Interdisciplinary Mathematics, 23: 493-502.

Saha, S. (2021a) Numerical simulation of turbulent flow through a sudden expansion channel: comparison between three models. Lecture notes in Mechanical Engineering, 49-56.

Saha, S. (2021b) A Survey on Flow Phenomena and Heat Transfer Through Expansion Geometry. Lecture Notes in Mechanical Engineering, 257-264.

Saha, S. & Das, N. A. (2021) Flow Bifurcation Phenomena of Shear-Thinning and Newtonian Fluids in a Rectangular Channel in Presence of Intermediate Steps: using Carreau-Yasuda Model. Journal of Applied Fluid Mechanics, 14 (4), 1283-1293.

Saha, S., Raut, S. & Das, N. A. (2021) Thermal enhancement and entropy generation of laminar water-Al2O3 nano-fluid flow through a sudden expansion channel with bell-shaped surface. International Journal of Fluid Mechanics Research, 48 (3): 65-78.

Saha, S. & Das, N. A. (2022) Hydro-thermal analysis of water-Al_2O_3 nanofluid flow through a sudden expansion channel with intermediate step. Kuwait Journal of Science, 49(4): 1-12.

Saha, S., Biswas, P., Das, N. A., Kumar, R. A. & Singh, K. M. (2023) Analysis of Blood Flow Bifurcation Phenomena in Mitral Valve: A Numerical Approach to Predict Cardiac Arrest Journal of Applied Fluid Mechanics, 16 (3), 491-504.

Sanmigue, R. E., Pino, C. &Gutie, M. C. (2010) Global mode analysis of a pipe flow through a 1:2 axisymmetric sudden expansions. Phys. Fluids, 22: 1-4.

Shapira, M., Degani, D. &Weihs, D. (1990) Stability and existence of multiple solutions for viscous flow in suddenly enlarged channels. Computers Fluids, 18: 239-258.

Soong, C.Y., Tzeng, Y. P. & Hsieh, D. C. (1998) Numerical investigation of flow structure and bifurcation phenomena of confined plane twin-jet flows. Phys. Fluids, 10: 2910-2921.

Terekhov, V. V. &Terekhov, I. V. (2017) Effect of surface permeability on the structure of a separated turbulent flow and heat transfer behind a backward-facing step. J ApplMech Tech Phys, 58: 254-263.

Ternik, P. (2010) New contributions on laminar flow of inelastic non-Newtonian fluid in the two-dimensional symmetric expansion: Creeping and slowly moving flow conditions. Journal of Non-Newtonian Fluid Mechanics, 165: 1400-1411.

Ternik, P. (2009) Planar sudden symmetric expansion flows and bifurcation phenomena of purely viscous shear-thinning fluids.Journal of Non-Newtonian Fluid Mechanics, 157(1-2):15-25.

Ternik, P., Marn, J. &Zunic, Z. (2006) Non-Newtonian Fluid Flow through a Planar Symmetric Expansion: Shear-thickening Fluids. Journal of Non-Newtonian Fluid Mechanics, 13: 136-148.

Thiruvengadam, M., Nie, H. J. &Armaly, F. B. (2005) Bifurcated three-dimensional forced convection in plane symmetric sudden expansion. International Journal of Heat and Mass Transfer, 48: 3128-3139.

Torres, M. J., Garca, J. & Doce, Y. (2020) Numerical Study of Particle Dispersion in the Turbulent Recirculation Zone of a Sudden Expansion Pipe using Stokes Numbers and Mean Drift Parameter. Journal of Applied Fluid Mechanics, 13: 15-23.

Van Doormaal, J.P. &Raithby, G.D. (1985) Enhancements of the SIMPLE method for predicting incompressible fluid flows, Numerical Heat Transfer, 7: 147-163.

Youcef, A., Saim, R., Oztop, H. & Ali, M. (2019) Turbulent forced convection in a shell and tube heat exchanger equipped with novel design of wing baffles, International Journal of Numerical Methods for Heat & Fluid Flow, 29(6): 2103-2127.

Youcef, A. & Saim, R. (2021) Numerical Analysis of the Baffles Inclination on Fluid Behavior in a Shell and Tube Heat Exchanger, J. Appl. Comput. Mech, 7(1): 312-320.

Submitted: 17/01/2022
Revised: 06/04/2022
Accepted: 17/04/2022
DOI : 10.48129/kjs.18147